

anato derivatives of the 1,7-diene isomers (mainly the 1,4-diene isomer) is ensured by recrystallization of the *dl* and *meso* (low spin) diastereoisomers from water. The dithiocyanato salt of the 1,4-diene isomer is several times more soluble in water at room temperature than is either of the dithiocyanato 1,7-diene isomers. This isomeric purity of the dithiocyanato isomers allows them to be the precursors for all other 1,7-diene derivatives.

dl- and *meso*-Ni(1,7-CT)(BF₄)₂. These salts are prepared by dissolving the appropriate isomer, *dl*- or *meso*-Ni(1,7-CT)(NCS)₂ (1.8 g), in 0.01 *N* HBF₄ (40 ml). Silver nitrate (1.5 g) dissolved in 20 ml of 0.01 *N* HBF₄ is added and the mixture is vigorously stirred. The AgSCN is filtered off and to the filtrate is added 15 ml of a saturated NaBF₄ solution. The volume is reduced to approximately 50 ml by passing a stream of air across the surface of the solution. The yellow product is isolated by filtration, washed with small amounts of cold 0.01 *N* HBF₄, and dried under vacuum desiccation (yield ~50%). *Anal.* Calcd for C₅H₃₂N₄B₂F₈Ni: C, 37.47; H, 6.29; N, 10.93. Found (*dl* isomer): C, 37.2; H, 6.86; N, 11.2. Found (*meso* isomer): C, 37.7; H, 6.36; N, 10.9.

dl- and *meso*-Ni(1,7-CT)(PF₆)₂. The appropriate diastereoisomer, *dl* or *meso*-Ni(1,7-CT)(NCS)₂ (2 g), is dissolved in 70 ml of 0.01 *N* HCl. To this solution is added with stirring 8 g of NH₄PF₆ in 20 ml of H₂O. The yellow microcrystalline product is isolated by filtration, washed with water, and dried in a vacuum desiccator (yield ~85%). *Anal.* Calcd for C₁₆H₃₂N₄P₂F₁₂Ni: C, 30.55; H, 5.13; N, 8.91; F, 36.24. Found (*dl* isomer): C, 30.71; H, 5.17; N, 8.95; F, 36.10. Found (*meso* isomer): C, 30.77; H, 5.20; N, 8.26; F, 36.05.

dl- and *meso*-Ni(1,7-CT)(ClO₄)₂. These derivatives are prepared following the procedure described for the preparation of the hexafluorophosphate derivatives; only perchloric acid and sodium perchlorate are substituted for HCl and NH₄PF₆, respectively. *Anal.* Calcd for C₁₆H₃₂N₄Cl₂O₈Ni: C, 35.71; H, 5.99; N, 10.41. Found (*dl* isomer): C, 35.8; H, 6.07; N, 10.7. Found (*meso* isomer): C, 35.6; H, 6.25; N, 10.59.

The isomeric purity of all derivatives of each isomer was determined using pmr spectroscopy. The only exception was the determination of possible 1,4-diene contamination in derivatives of the *dl*-1,7-diene isomer.

It should be noted that prolonged contact of any of the derivatives of either the *dl*- or *meso*-1,7-diene isomers with neutral aqueous solutions results in isomerization and equilibration of these two diastereoisomers.

Deuteration Experiments. Deuteration of the Ni(1,4-CT)²⁺ isomer was accomplished by dissolving any of its salts in basic D₂O. This accomplished the deuteration of the secondary amine, the imine methyl group, and the methylene function of the six-membered

chelate rings within a few minutes, as was evident from the pmr spectrum of each such solution. No solid deuterated derivatives of this isomer were isolated.

Two recrystallizations of the *dl*-Ni(1,7-CT)(BF₄)₂ isomer from D₂O resulted in deuteration of only the secondary amines. The infrared spectrum of the deuterated complex showed $\nu(N-D)$ bands at 2410 and 2390 cm⁻¹ ($\nu(N-D)/\nu(N-H) = 1.34$). Relative areas of the $\nu(N-D)$ and $\nu(N-H)$ bands indicated at least 90% deuteration of the amine function. The absence of any $\nu(C-D)$ bands in the 2100–2300-cm⁻¹ region of the infrared spectrum indicated the absence of any further deuteration. This sample was found to be free of the *meso* diastereoisomer as indicated from its pmr spectrum shown in Figure 4B.

Deuteration of the secondary amines, imine methyl groups, and the methylene function of the six-membered chelate rings of the *dl*-Ni(1,7-CT)(BF₄)₂ isomer was accomplished by twice recrystallizing from D₂O made basic with 4 *N* NaOH (pH 10 as indicated on Fisher Alkacid Test Ribbon). The infrared spectrum showed $\nu(N-D)$ bands at 2410 and 2390 cm⁻¹ and at least 90% deuteration of the amine functions. A $\nu(C-D)$ band centered at 2200 cm⁻¹ was also present and accompanied by gross changes in the $\nu(C-H)$ region centered at 2930 cm⁻¹ ($\nu(C-H)/\nu(C-D) = 1.33$) and in the finger-print region, 1200–1500 cm⁻¹. This sample was free of the *meso*-1,7-diene isomer as indicated by its pmr spectrum. The pmr spectrum shown in Figure 4C was obtained using this sample.

Tris(ethylenediamine)nickel(II) fluoroborate was condensed with acetone-*d*₆ and the deuterated product, *dl*-Ni(1,7-CT)(BF₄)₂, was isolated as described above and then recrystallized from D₂O. This product has all proton positions deuterated except those of the dimethylene chains which constitute the five-membered chelate rings. *Anal.* Calcd for C₁₆H₈D₂₄N₄B₂F₈Ni: C, 35.79; H (D), 6.48; N, 10.44; F, 28.31. Found: C, 35.72; H (D), 6.45; N, 10.52; F, 28.15.

The infrared spectrum of this *dl*-Ni(1,7-CT)(BF₄)₂-*d*₂₄ confirms the deuteration of the amine functions and some of the C-H positions: $\nu(ND)$ 2400 br, $\nu(C-D)$ 2230 cm⁻¹. The pmr spectrum confirms the deuteration of all methyl and methylene positions. The 2.5–4.5-ppm region of this spectrum is identical with that spectrum shown in Figure 4C, thus confirming the extent of the previously described deuteration.

Acknowledgment. This investigation was supported in part by the National Science Foundation and by U.S. Public Health Service Grant GM 10040. This support is sincerely appreciated. Public Health Service Fellowships 1-F2-GM-28, 191-01, and 4-F2-GM-28, 191-02 are also gratefully acknowledged (N. J. R.).

Spin-Delocalization Mechanisms in Some Paramagnetic Tris-2,2'-bipyridine Complexes of Nickel(II)¹

M. Wicholas and R. S. Drago

Contribution from the William A. Noyes Laboratory, University of Illinois, Urbana, Illinois. Received February 15, 1968

Abstract: The proton nmr contact shifts of Ni(bipy)₃²⁺ (bipy = 2,2'-bipyridine) and some substituted bipyridine complexes are reported, and the mechanisms of unpaired electron spin delocalization in these complexes are discussed. It is found that both σ - and π -delocalization mechanisms are important. The shifts can be interpreted quantitatively by comparing the experimental contact shifts with those predicted from extended Hückel molecular orbital calculations. These results and the change in direction of the shifts on substituting CH₃ for H at various ring positions are employed to indicate which ligand MO's are most extensively mixed with the metal ion in the MO's containing unpaired electrons.

In this laboratory we have been interested in the nmr contact shifts of paramagnetic transition metal complexes and in their use in the elucidation of the nature of metal-ligand bonding. From a simple ob-

servation of the shifts of different protons in a ligand, one can often infer whether or not spin delocalized in a

(1) Abstracted in part from the Ph.D. thesis of M. Wicholas, University of Illinois, 1967.

σ or π molecular orbital of the ligand is the dominant mechanism. However, it often becomes difficult to interpret the shifts in a given complex in terms of only metal-ligand π or σ bonding. We have recently shown² that, contrary to what has often been inferred, π delocalization in a ligand does not necessarily imply metal-ligand π bonding. There is hope of obtaining quantitative information about the delocalization mechanisms and information about metal-ligand bonding by carrying out extended Hückel molecular orbital calculations on the ligand and by varying the central metal ion in a series of complexes with a given ligand. We are encouraged to try to calculate contact shifts with the EH method in view of the success recently reported for calculating proton and nitrogen epr hyperfine coupling constants for a series of organic free radicals.³⁻⁵

For this study we have selected a series of substituted and unsubstituted trisbipyridylnickel(II) complexes. The rigidity of the chelate structure is advantageous for extended Hückel calculations. Some of the complications introduced when the ligand can undergo free rotation have been discussed.⁶ Furthermore, the diversity of transition metal ion complexes that can be prepared with this ligand should permit a thorough investigation of the problems described above.

An earlier report⁷ based on unpublished data has stated that the contact shifts in $\text{Ni}(\text{bipy})_3^{2+}$ attenuate, indicating σ delocalization of the unpaired electrons. Since it seemed to us very unusual for σ delocalization alone to be responsible for the contact shifts, especially in light of the studies done with some substituted pyridine complexes,⁸⁻¹¹ this provided added incentive to examine in detail the contact shifts of a series of tris-(2,2'-bipyridine) complexes. The results of this study show that one can sometimes be misled by trying to infer spin-delocalization mechanisms by qualitatively looking at the trend in shifts of various protons in a ligand. Indeed, we present evidence here to indicate a significant contribution to spin delocalization from ligand π molecular orbitals.

Experimental Section

Materials and Analyses. 2,2'-Bipyridine was purchased from Eastman Organic Chemicals while the methyl- and phenyl-substituted bipyridines were purchased from G. Frederick Smith Co., except for 5,5'-dimethyl-2,2'-bipyridine which was synthesized by the procedure of Sasse and Whittle.¹² All other reagents and solvents were commercially available.

Preparation of the Complexes. In the following syntheses and throughout the text, the substituted bipyridine ligands shall be abbreviated as follows: 2,2'-bipyridine = bipy; 4,4'-dimethyl-2,2'-bipyridine = 4,4'-(CH₃)₂bipy; 5,5'-dimethyl-2,2'-bipyridine = 5,5'-(CH₃)₂bipy; 4,4'-diphenyl-2,2'-bipyridine = 4,4'-(C₆H₅)₂bipy.

M(bipy)₃Cl₂·nH₂O (M = Fe(II), Ni(II)). These complexes were prepared by the method of Inskeep.¹³ The hydrated metal chloro-

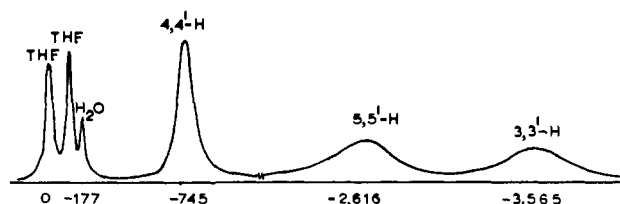


Figure 1. Nmr spectrum of $\text{Ni}(\text{bipy})_3\text{Cl}_2 \cdot 2\text{H}_2\text{O}$ in D_2O .

ride was dissolved in a minimum amount of water, and the solution was heated with a stoichiometric amount of 2,2'-bipyridine. Upon cooling crystals were formed and these were filtered and washed with ice-cold water. The product was dried *in vacuo* over P_2O_5 . For future reference, this method of preparation shall be called the aqueous method.

Anal. Calcd for $\text{Ni}(\text{C}_{10}\text{H}_8\text{N}_2)_3\text{Cl}_2 \cdot 2\text{H}_2\text{O}$: C, 56.81; H, 4.45; N, 13.25. Found: C, 56.91; H, 4.26; N, 13.10. Calcd for $\text{Fe}(\text{C}_{10}\text{H}_8\text{N}_2)_3\text{Cl}_2 \cdot 2\text{H}_2\text{O}$: C, 57.06; H, 4.47; N, 13.31. Found: C, 57.40; H, 4.45; N, 13.11.

M(5,5'-(CH₃)₂bipy)₃Cl₂·2H₂O (M = Fe(II), Ni(II)). Both the nickel(II) and iron(II) hydrated metal chlorides were dissolved in a minimum amount of methanol, and the solution was heated with a stoichiometric amount of the ligand. Tetrahydrofuran (THF) was added until a slight turbidity was noticed. The solution was then allowed to cool and the crystals were filtered, washed with tetrahydrofuran, and dried *in vacuo* over P_2O_5 .

Anal. Calcd for $\text{Ni}(\text{C}_{12}\text{H}_{12}\text{N}_2)_3\text{Cl}_2 \cdot 1.5\text{H}_2\text{O}$: C, 60.96; H, 5.54; N, 11.85. Found: C, 60.82; H, 5.47; N, 11.39. Calcd for $\text{Fe}(\text{C}_{12}\text{H}_{12}\text{N}_2)_3\text{Cl}_2 \cdot 3.5\text{H}_2\text{O}$: C, 58.23; H, 5.84; N, 11.32. Found: C, 58.39; H, 5.38; N, 11.39.

M(4,4'-(CH₃)₂bipy)₃Cl₂·2H₂O (M = Fe(II), Ni(II)). These complexes were prepared by the aqueous method.

Anal. Calcd for $\text{Ni}(\text{C}_{12}\text{H}_{12}\text{N}_2)_3\text{Cl}_2 \cdot \text{H}_2\text{O}$: C, 61.74; H, 5.47; N, 12.01. Found: C, 61.84; H, 5.80; N, 11.05. Calcd for $\text{Fe}(\text{C}_{12}\text{H}_{12}\text{N}_2)_3\text{Cl}_2 \cdot 2\text{H}_2\text{O}$: C, 60.44; H, 5.64; N, 11.75. Found: C, 60.79; H, 5.65; N, 11.95.

Ni(4,4'-(C₆H₅)₂bipy)₃(NO₃)₂·H₂O. Nickel nitrate hexahydrate was dissolved in a minimum amount of hot acetone, and a stoichiometric amount of ligand was added. The solution was stirred and quickly decanted, thus removing any excess ligand before crystallization of the complex occurred. The solution was then cooled, and the resultant orange microcrystalline solid was filtered, washed with acetone, and dried *in vacuo* over P_2O_5 .

Anal. Calcd for $\text{Ni}(\text{C}_{22}\text{H}_{16}\text{N}_2)_3(\text{NO}_3)_2 \cdot \text{H}_2\text{O}$: C, 70.40, H, 4.48; N, 9.95. Found: C, 70.05; H, 4.76; N, 9.19.

Spectral Measurements. The nmr spectra were obtained with a Varian DP-60 and a Jeolco C60-H spectrometer. All shifts in deuteriochloroform are reported relative to tetramethylsilane (TMS) as an internal reference whereas all shifts in D_2O were measured relative to the high-field multiplet of tetrahydrofuran (THF) which was used as an internal reference.

Results and Discussion

Assignment of Nmr Bands. The isotropic shifts of the 2,2'-bipyridine complexes prepared here are listed in Table I, and the chemical shifts of the protons of the diamagnetic references are listed in Table II. The nmr spectra of the nickel(II) bipyridine complexes were assigned on the basis of line widths and methyl substitution of 2,2'-bipyridine. For example, the nmr spectrum of $\text{Ni}(\text{bipy})_3\text{Cl}_2 \cdot 2\text{H}_2\text{O}$ in D_2O (Figure 1) shows four resonance peaks (not including that of H_2O) which are attributable to the ligand protons. The 6,6'- and 4,4'-proton resonances are readily identified because of their line widths. The 6,6'-proton resonance has the largest half-width because of the proximity of these protons to the metal ion, and the 4,4'-proton resonance has the smallest half-width because these protons are most distant from the metal ion. The two remaining peaks at -2673 and -3670 cps are attributable to the 5,5'- and 3,3'-proton resonances and have similar half-

(13) R. Inskeep, *J. Inorg. Nucl. Chem.*, **24**, 763 (1962).

(2) R. J. Fitzgerald and R. S. Drago, *J. Am. Chem. Soc.*, **89**, 2879 (1967).

(3) R. S. Drago and H. Petersen, Jr., *ibid.*, **89**, 5774 (1967).

(4) R. S. Drago and H. Petersen, Jr., *ibid.*, **89**, 3978 (1967).

(5) R. E. Cramer and R. S. Drago, *ibid.*, **90**, 4790 (1968).

(6) R. J. Fitzgerald and R. S. Drago, *ibid.*, **90**, 2523 (1968).

(7) D. R. Eaton and W. D. Phillips, *Advan. Magnetic Resonance*, **1**, 103 (1965).

(8) J. A. Happe and R. L. Ward, *J. Chem. Phys.*, **39**, 1211 (1963).

(9) R. H. Holm, G. W. Everett, Jr., and W. D. Horrocks, Jr., *J. Am. Chem. Soc.*, **88**, 1071 (1966).

(10) B. B. Wayland and R. S. Drago, *ibid.*, **88**, 4597 (1966).

(11) G. N. LaMar, *Inorg. Chem.*, **6**, 1939 (1967).

(12) W. H. F. Sasse and C. P. Whittle, *J. Chem. Soc.*, 1347 (1961).

Table I. Contact Shifts of the Bipyridine Complexes

Compound	Solvent	$\Delta\nu_{6,6'}$	$\Delta\nu_{5,5'}$	$\Delta\nu_{4,4'}$	$\Delta\nu_{3,3'}$	ν_{H_2O}
Ni(bipy) ₃ Cl ₂ ·2H ₂ O	D ₂ O	-7694	-2294	-363	-3151	-284
Ni(5,5'-(CH ₃) ₂ bipy) ₃ Cl ₂ ·1.5H ₂ O	D ₂ O	-9900 ^a	-359	-306	-3121	-288
Ni(4,4'-(CH ₃) ₂ bipy) ₃ Cl ₂ ·H ₂ O	D ₂ O		-2276	+607	-3100	-289
Ni(4,4'-(C ₆ H ₅) ₂ bipy) ₃ (NO ₃) ₂ ·H ₂ O	CDCl ₃		-2670	(-69, +60)	-3288	

^a This resonance was measured on the oscilloscope and is accurate to only ± 1000 cps.

Table II. Chemical Shifts of the Diamagnetic Bipyridine References

Compound ^{a,b}	Solvent	$\nu_{6,6'}$	$\nu_{5,5'}$	$\nu_{4,4'}$	$\nu_{3,3'}$	ν_{H_2O}
Fe(bipy) ₃ Cl ₂ ·2H ₂ O	D ₂ O	-446	-446	-489	-519	-280
Fe(5,5'-(CH ₃) ₂ bipy) ₃ Cl ₂ ·3.5H ₂ O	D ₂ O	-435	-132	-479	-511	-286
Fe(4,4'-(CH ₃) ₂ bipy) ₃ Cl ₂ ·2H ₂ O	D ₂ O	-439	-439	-152	-513	-288
4,4'-(C ₆ H ₅) ₂ bipy	CDCl ₃	-540	-480	-465	-542	

^a All shifts are reported relative to TMS in cps. The shifts in aqueous solution were measured relative to the high-field multiplet of THF and were converted to TMS using τ of THF = 8.22. ^b The assignments were made with the aid of the previously published chemical shift assignments for 2,2'-bipyridine and some of its diamagnetic complexes: S. Castellano, H. Gunther, and S. E. Bersole, *J. Phys. Chem.*, **69**, 4166 (1965); F. A. Kramer, Jr. and R. West, *ibid.*, **69**, 673 (1965).

widths. These can readily be distinguished by comparing the proton nmr resonances of Ni(bipy)₃Cl₂·2H₂O and Ni(5,5'-(CH₃)₂bipy)₃Cl₂·1.5H₂O, for it is found that methyl substitution causes very little change in the proton resonances of the other ring protons compared to the position of the analogous protons in Ni(bipy)₃Cl₂·2H₂O. The water resonance could easily be distinguished from ligand proton resonances, by the addition of water and comparison of the relative peak areas of samples with and without water added. Since the ground state of nickel(II) in D₃ symmetry is orbitally nondegenerate, the complexes reported here are expected to have no significant pseudo-contact shifts and their measured shifts are attributable to contact shifts. Consequently, the shifts provide direct information regarding the mechanisms of spin delocalization. The contact shifts for Ni(bipy)₃²⁺ (Table I) are all downfield and show attenuation and as such imply that a σ delocalization mechanism is operative. For a σ mechanism one would expect the following to be true of the proton contact shifts: $|\Delta\nu_{6,6'}| > |\Delta\nu_{3,3'}| > |\Delta\nu_{5,5'}| > |\Delta\nu_{4,4'}|$. Although the observed contact shifts for Ni(bipy)₃²⁺ follow this order, the contact shifts for Ni(4,4'-(CH₃)₂bipy)₃²⁺ provide excellent evidence for the participation of a π mechanism along with the dominant σ mechanism in delocalization of unpaired spin in the ligand. In the latter $\Delta\nu_{CH_3} = +607$ cps, and the large upfield contact shift must result from π delocalization of unpaired spin.¹⁴

A modified extended Hückel molecular orbital calculation (EHMO)¹⁵ was attempted for 2,2'-bipyridine. All atomic orbital input parameters have been described previously.³ Bond angles and lengths for 2,2'-bipyridine were estimated using the structural parameters for [Cu(bipy)₂]I¹⁶ in which the ring dimensions are the same as in free bipyridyl. The energies of the resultant molecular orbitals are listed in Table III. ψ_6 is the highest occupied molecular orbital and is of σ symmetry. In Table IV the eigenvector coefficients of the more important molecular orbitals (ψ_4 , ψ_5 , ψ_6 , ψ_7 , and ψ_8) are

(14) A. D. McLachlan, *Mol. Phys.*, **1**, 233 (1958).

(15) P. C. Van Der Voorn and R. S. Drago, *J. Am. Chem. Soc.*, **88**, 3255 (1966).

(16) G. A. Barclay, B. W. Hoskins, and C. H. L. Kennard, *J. Chem. Soc.*, 5691 (1963).

listed. For π orbitals the gross atomic populations (*i.e.*, $C_j^2 + \sum_i C_i C_j S_{ij}$; charge densities) have been shown to correspond to epr hyperfine coupling constants. We have listed these values for the π molecular orbitals ψ_4 , ψ_7 , and ψ_8 in Table V.

Table III. Molecular Orbital Energies of 2,2'-Bipyridine

Molecular orbital ^{a,b}	Energy, eV	Molecular orbital ^{a,b}	Energy, eV
ψ_9 (π^* , e)	-8.682	ψ_4 (π , a ₁ + e)	-12.392
ψ_8 (π^* , a ₁ + e)	-8.687	ψ_3 (π , a ₁ + e)	-12.830
ψ_7 (π^* , e)	-9.303	ψ_2 (π , e)	-12.871
ψ_6 (σ (a ₂ + e)	-11.280	ψ_1 (σ)	-13.057
ψ_5 (σ (a ₁ + e)	-11.340		

^a The first term in the parentheses indicates the symmetry of the ligand molecular orbital. The second term indicates the metal d orbitals which have approximate symmetry to combine with the π and π^* orbitals. For the π and π^* orbitals, the symmetries of the metal orbitals with which the ligand orbital may combine are listed assuming the complexes formed are of D₃ symmetry. ^b ψ_6 is the highest filled molecular orbital.

With respect to π bonding there are two types of ligand π molecular orbitals in D₃ symmetry: those which can combine with metal e orbitals and those which can combine with both metal e and a₁ orbitals. In D₃ symmetry the d orbitals are split as follows: $t_{2g} \rightarrow 1e + 1a_1$ and $e_g \rightarrow 2e$. Using a point dipole approximation, Orgel¹⁷ found that the 1a₁ orbital is lowest in energy for a flattened D₃ arrangement and the 1e orbital is lowest for an elongated octahedral arrangement. This treatment, however, neglects π bonding; hence, it is quite uncertain then whether the 1a₁ or 1e orbital is lowest in energy in these bipyridine complexes. In the nickel(II) complexes the two unpaired electrons are in the 2e orbitals.

We first consider the plausibility of explaining the contact shifts solely by means of a σ mechanism. In a σ -delocalization mechanism for Ni(bipy)₃²⁺, one would expect the 2e orbitals on nickel to overlap with $\psi_6(\sigma)$ or $\psi_5(\sigma)$ or both and thus transmit positive spin directly onto the ligand protons *via* the ligand σ MO (s). Nega-

(17) L. E. Orgel, *ibid.*, 3683 (1961).

Table IV. Molecular Orbital Coefficients for 2,2'-Bipyridine

Orbital	Coefficients ^a		Orbital	Coefficients ^a		
	ψ_6	ψ_5		ψ_4	ψ_7	ψ_8
C _{6'} (s)	-0.0149	-0.0276*	C _{6'} (p _z)	-0.1306	-0.0327*	-0.4021
(p _x)	0.0863	0.1283*	C _{5'} (p _z)	-0.3689	-0.3732*	0.0182*
(p _y)	0.0819*	0.0762	C _{4'} (p _z)	-0.1512	0.2873	0.4022*
C _{5'} (s)	0.0407*	0.0385	C _{3'} (p _z)	0.2464*	0.1879	-0.3564
(p _x)	-0.0752*	-0.0784	C _{2'} (p _z)	0.3508*	-0.3791*	-0.0937
(p _y)	-0.1487	-0.1372*	N (p _z)	0.3023*	0.4760	0.4511*
C _{4'} (s)	-0.0044	-0.0168*				
(p _x)	0.0013	0.0508*				
(p _y)	0.0327*	0.0297				
C _{3'} (s)	0.0369*	0.0404				
(p _x)	-0.0754*	-0.1124				
(p _y)	-0.1386	-0.1373*				
C _{2'} (s)	0.0018*	-0.0517*				
(p _x)	-0.0466*	0.1424*				
(p _y)	0.1281*	0.1196				
N (s)	0.1383*	0.1492				
(p _x)	-0.2980*	-0.3508				
(p _y)	-0.5482	-0.4870*				
H _{6'} (s)	-0.0825	-0.0572*				
H _{5'} (s)	-0.0381	-0.0576*				
H _{4'} (s)	0.0752*	0.0847				
H _{3'} (s)	-0.0520	-0.0314*				

^a An asterisk indicates that the sign of the coefficient of the corresponding unlisted orbital on the other ring is negative.

Table V. Gross Atomic Populations for 2,2'-Bipyridine

Atomic orbital	ψ_4	ψ_7	ψ_8
C _{6,6'} (p π)	0.0376	0.0017	0.2399
C _{5,5'}	0.3073	0.2235	0.0006
C _{4,4'}	0.0518	0.1327	0.2457
C _{3,3'}	0.1351	0.0580	0.1920
C _{2,2'}	0.2650	0.2197	0.0129
N	0.2033	0.3645	0.3091

tive contact shifts (downfield shifts) would thus result. In a σ mechanism one is interested in the unpaired electron density at the hydrogen nuclei or, more directly, the value of ψ^2 at the nucleus of concern, where ψ is the eigenvector of the molecular orbital in which the unpaired electron is delocalized. The value of ψ_j at the point (p) is given by $\sum_j C_{ij} \phi_j(p)$, where C_{ij} is the coefficient of atomic orbital ϕ_i in molecular orbital ψ_j . The numerical values of C_{ij} are taken from the EHMO calculation, and from these $\psi_j^2(p)$ is evaluated at the proton.³ Finally $\psi_j^2(p)$ is proportional to the electron-nuclear spin coupling constant for a proton located at position p . Delocalization of an unpaired spin into ψ_6 via a σ mechanism produces the following values for ψ_6^2 at the four sets of protons in 2,2'-bipyridine: $\psi_6^2(6,6') = 4.147 \times 10^{-3}$, $\psi_6^2(5,5') = 1.156 \times 10^{-3}$, $\psi_6^2(4,4') = 3.239 \times 10^{-3}$, and $\psi_6^2(3,3') = 2.062 \times 10^{-3}$. The value of $\psi_6^2(4,4')$ is too high, for one would expect considerable attenuation of the spin density on an atom so many bonds removed from the nitrogen. Delocalization by a σ mechanism into ψ_5 gives values of $\psi_5^2(6,6') = 1.905 \times 10^{-3}$, $\psi_5^2(5,5') = 2.345 \times 10^{-3}$, $\psi_5^2(4,4') = 4.338 \times 10^{-3}$, and $\psi_5^2(3,3') = 8.028 \times 10^{-4}$.

The high values calculated for $\psi_6^2(4,4')$ and $\psi_5^2(4,4')$ should be discussed. The same problem is encountered in comparing the extended Hückel calculation for pyridine with the contact shifts in Ni(C₅H₅N)₂I₂, Ni(C₅H₅N)₂(NO₃)₂, or Ni(C₅H₅N)₆²⁺. In pyridine, a ligand very closely related to 2,2'-bipyridine, $\psi_\sigma^2(\gamma)$, is much too high. It is interesting to note that this

γ proton in pyridine is located in a position relative to nitrogen which is comparable to the 4,4' protons in 2,2-bipyridine. For Ni(C₅H₅N)₂I₂, Holm, *et al.*,⁹ report that $\Delta\nu_\beta/\Delta\nu_\alpha = 0.297$ and $\Delta\nu_\gamma/\Delta\nu_\alpha = 0.0664$ while for Ni(C₅H₅N)₂(NO₃)₂ Rosenthal¹⁸ reports that $\Delta\nu_\beta/\Delta\nu_\alpha = 0.278$ and $\Delta\nu_\gamma/\Delta\nu_\alpha = 0.0911$. For Ni(C₅H₅N)₆²⁺, which exists in nitromethane solutions in the presence of excess pyridine,^{18,19} $\Delta\nu_\gamma/\Delta\nu_\alpha = 0.398$ and $\Delta\nu_\beta/\Delta\nu_\alpha = 0.156$. On the basis of an extended Hückel calculation, Holm and coworkers⁹ calculate that $\Delta\nu_\beta/\Delta\nu_\alpha = 0.297$ and $\Delta\nu_\gamma/\Delta\nu_\alpha = 1.97$. There seems to be some unknown inadequacy in the extended Hückel calculation for an atom on the line bisecting the nucleus and the atomic orbital containing most of the unpaired spin density. Recent molecular orbital calculations on the phenyl radical support this claim. The esr spectrum of the phenyl radical, which is isoelectronic with pyridine, has been measured,²⁰ and the coupling constants in the gauss are: $A_\alpha = 19.5$, $A_\beta = 6.5$, and $A_\gamma \cong 0$. Extended Hückel calculations^{21,22} and a modified hyperconjugation calculation²³ both predict large γ -proton coupling constants. For example, Petersen²¹ calculates values of $A_\alpha = 18.1$, $A_\beta = 5.47$, and $A_\gamma = 6.22$; Petersson and McLachlan²² predict that $A_\alpha = 12.5$, $A_\beta = 5.3$, and $A_\gamma = 11.0$; and Dixon²³ predicts that $A_\alpha = 23.3$, $A_\beta = 4.2$, and $A_\gamma = 17.9$. Atherton and Hinchliffe,²⁴ using the unrestricted Hartree-Fock method with complete neglect of differential overlap (CNDO), are the first to correctly predict the near-zero γ -proton coupling constant, and they find that $A_\alpha = 23.73$, $A_\beta = 6.62$, and $A_\gamma = 0$. These results lend credence to the belief that the extended Hückel calculation yields inaccurate highest filled σ -orbital coefficients at the γ proton in pyridine

(18) M. Rosenthal, Ph.D. Thesis, University of Illinois, 1965.

(19) M. R. Rosenthal and R. S. Drago, *Inorg. Chem.*, **4**, 840 (1965).

(20) J. E. Bennett, B. Mile, and A. Thomas, *Chem. Commun.*, 265 (1965).

(21) H. Petersen, Ph.D. Thesis, University of Illinois, 1967.

(22) G. A. Petersson and A. D. McLachlan, *J. Chem. Phys.*, **45**, 628 (1966).

(23) W. T. Dixon, *Mol. Phys.*, **9**, 201 (1965).

(24) N. M. Atherton and A. Hinchliffe, *ibid.*, **12**, 349 (1967).

and at the 4,4' protons in 2,2'-bipyridine. In both cases ψ_{σ}^{2s} 's for these protons are much too high. However, correct values for $\psi_{\sigma}(\alpha)^2$ and $\psi_{\sigma}(\beta)^2$ can be obtained in phenyl and probably pyridine. Therefore, we have confidence in the values calculated for the σ MO's at proton positions in bipyridine other than 4,4'.

As was previously mentioned, a reversal in the sign of the methyl proton contact shift for $\text{Ni}(4,4'-(\text{CH}_3)_2\text{bipy})_3^{2+}$ compared to the 4,4'-proton contact shift in $\text{Ni}(\text{bipy})_3^{2+}$ indicates that some π delocalization occurs in these bipyridine complexes. In fact, it is very likely that the 4,4'-methyl proton contact shift is entirely due to π delocalization since σ contact shifts attenuate rapidly with increasing bond separation from the metal ion.

The π overlap of ψ_4 with the metal 2e orbitals delocalizes positive spin in ψ_4 which will cause a (upfield) methyl contact shift in $\text{Ni}(4,4'-(\text{CH}_3)_2\text{bipy})_3^{2+}$ because of the small value of the charge density at the 4,4'-carbon $2p_x(\pi)$ atomic orbitals (Table V). At both the 6,6'- and 4,4'-carbon $2p(\pi)$ atomic orbitals in ψ_4 , delocalization of positive spin density into ψ_4 could result in negative spin density at the 6,6'- and 4,4'-carbon $2p_x(\pi)$ positions by spin polarization. This involves polarization of filled π orbitals by a mechanism similar to that which produces negative spin density at the central carbon in the allyl radical. This will produce downfield contact shifts for the 6,6' and 4,4' protons in $\text{Ni}(\text{bipy})_3^{2+}$ and upfield contact shifts for the 4,4'-methyl protons in $\text{Ni}(4,4'-(\text{CH}_3)_2\text{bipy})_3^{2+}$. The plausibility of this mechanism rests upon the assumption that spin polarization will dominate direct delocalization at the 4,4'-carbon $2p_x(\pi)$ position. The small value of the charge density (0.0518) makes this conclusion reasonable, but it is not known whether spin polarization or direct delocalization will dominate.

One can immediately disqualify the transfer of positive spin onto ψ_7 by π overlap of the ψ_7 and 2e orbital. Contrary to what is observed, this overlap would result in a downfield contact shift for the 4,4'-methyl protons because the 4,4'-carbon $2p_x(\pi)$ atomic orbitals have large gross atomic populations in ψ_7 . There are two other plausible mechanisms, and these involve spin polarization of the paired $1a_1$ or $1e$ electrons by the unpaired 2e electrons. Negative spin density could be placed in the empty π^* orbital ψ_7 or filled ψ_4 by the partial unpairing of the essentially metal ion $1e$ electrons while negative spin density would result in ψ_8 (the next highest π^* orbital) from the partial unpairing of the $1a_1$ or $1e$ electrons. Delocalization into either ψ_7 or ψ_8 results in a π mechanism which would produce

the observed reversal in sign of proton and methyl proton contact shifts at the 4,4' positions.

It is of interest to now inquire which if any of the two spin polarization mechanisms involving ψ_7 and ψ_8 or the direct overlap mechanism involving ψ_4 can account for the negative (downfield) methyl proton contact shift in $\text{Ni}(5,5'-(\text{CH}_3)_2\text{bipy})_3^{2+}$. Delocalization of positive spin in ψ_4 produces a downfield 5,5'-methyl proton contact shift, while delocalization of negative spin in ψ_8 also produces a downfield 5,5'-methyl proton contact shift because of the node in ψ_8 at the 5,5'-carbon $2p_x(\pi)$ atomic orbitals (Table V). Delocalization of negative spin in ψ_7 , on the other hand, produces an upfield methyl proton contact shift, and, if the ψ_7 mechanism were operative, it would require that the competing σ mechanism dominate the contact shift for these methyl protons. It seems therefore that delocalizations of positive spin into ψ_4 or negative spin into ψ_7 and ψ_8 are reasonable π mechanisms for explaining π delocalization in the nickel(II) bipyridine complexes. On the basis of these qualitative arguments, it is impossible to choose between the alternative mechanisms for π delocalization.

Contact shifts have also been measured for the water-insoluble $\text{Ni}(4,4'-(\text{C}_6\text{H}_5)_2\text{bipy})_3(\text{NO}_3)_2 \cdot \text{H}_2\text{O}$ in CDCl_3 . The 6,6', 5,5', and 3,3' protons are easily identified and the remaining two peaks in the nmr attributed to the phenyl protons. Of these, an asymmetric peak with a slight shoulder is found at -534 cps from TMS, and a symmetric peak is found at -405 cps. The ratio of the areas underneath the peaks is 3:2 with the asymmetric peak being of larger area. The asymmetric peak must represent the resonances of two sets of protons, of which one is due to the *para* protons. The contact shifts for these protons are -69 cps, whereas the contact shift for the protons represented by the symmetric peak is $+60$ cps. The assignments for these proton resonances unfortunately cannot be unequivocally made. The downfield resonance peak is due to either the *ortho* and *para* protons or the *meta* and *para* protons, and for the upfield peak only one assignment is reasonable. It is proposed that the peak at -534 cps is due to the *ortho* and *para* protons, while that at -405 cps is due to the *meta* protons. The contact shifts are then: $\Delta\nu_{ortho} = -68$, $\Delta\nu_{meta} = +60$, and $\Delta\nu_{para} = -69$. If the assignments are correct, the contact shifts are consistent with π delocalization of positive spin density, involving ψ_4 .

Acknowledgment. The authors acknowledge the financial support of the National Science Foundation through Grant No. 5498.